JOURNAL OF AGRICULTURAL AND FOOD CHEMISTRY

Article

pubs.acs.org/JAFC

Cell Wall Polysaccharide Chemistry of Peach Genotypes with Contrasted Textures and Other Fruit Traits

Marc Lahaye,*[,†] Xavier Falourd,[†] Bernard Quemener,[†] Marie Christine Ralet,[†] Werner Howad,[‡] Elisabeth Dirlewanger,[§] and Pere Arús[‡]

[†]INRA, UR1268 Biopolymères Interactions Assemblages, BP 71627, F-44316 Nantes, France

[‡]IRTA, Centre de Recerca en Agrigenòmica CSIC-IRTA-UAB-UB, Campus UAB, Cerdanyola del Vallès (Bellaterra), 08193 Barcelona, Spain

[§]INRA, UR419 Espèces Fruitières, BP 81, F-33883 Villenave d'Ornon, France

Supporting Information

ABSTRACT: Cell wall composition, pectin, and hemicellulose fine structure variation were assessed in peach and related genotypes with contrasted texture and fruit shape. Cell walls were prepared from four commercial peaches, eight genotypes from the Jalousia × Fantasia peach cross, and six genotypes from the Earlygold peach × Texas almond cross. Sugar composition was determined chemically while fine structure of homogalacturonan pectin and xyloglucan hemicellulose were assessed by coupling pectin lyase and glucanase degradation, respectively, with MALDI-TOF MS analysis of the degradation products. The results indicate clear compositional and structural differences between the parents and their related genotypes on the basis of pectin versus cellulose/hemicellulose content and on the fine structure of homogalacturonan and xyloglucan. A relation between methyl- and acetyl-esterification of pectin with fruit shape is revealed in the Fantasia × Jalousia peach genotypes.

KEYWORDS: *cell wall, hemicellulose, xyloglucan, pectin, homogalacturonan, pectin lyase, glucanase, MALDI-TOF MS, texture, fruit shape*

INTRODUCTION

Fleshy fruit quality embraces a large panel of characteristics, such as color, taste, aroma, size, shape, and texture. Among these, texture is one of the major quality issues for breeders, growers, retailers, processors, and consumers. Texture encompasses sensory and mechanical aspects.[1] It relies on combinations of several structural determinants involving, at the tissue scale, cellular structure and, at the cellular scale, cell wall as well as turgor pressure.[2] Fruit size results from both cell division and cell expansion factors while shape involves the regulated development of the constitutive fruit tissues that likely combines cell wall factors and cell mechanical perception.[3,4] The setting up and evolution of these determinants of quality during fruit development and ripening are yet to be fully identified. Such basic knowledge is required to develop strategies for controlling fruit quality all along production, storage, and processing, and for breeding new varieties with desired characteristics. Systems biology and genetic approaches have been engaged in the aim of designing fruit genotypes with chosen shape and texture.[5−9] Due to the great complexity and interplay of the many cellular factors involved in these traits, such studies imply measurements of specific molecular and structural determinants at different scales among which cell walls are pivotal. Their intrinsic mechanical and adhesive characteristics contribute to the control of cell development, to the cellular cohesion in tissue, and to the viscoelastic characteristics of the tissue. Fleshy fruit cell walls have been the focus of many biochemical studies in relation with fruit softening and texture disorders.[10,11] They revealed cell wall reshuffling and disassembly mechanisms through particular sets of enzymes and proteins mostly triggered in climacteric fruit by the ethylene crisis at the onset of ripening. The variability of the chemical structures of cell wall polysaccharides related to genetic or developmental factors can conveniently be assessed through coupling specific enzymatic degradations and MALDI-TOF MS or HPLC analysis of the oligosaccharides produced.[12,13] This approach was successful in revealing cell wall polysaccharide structural changes in near isogenic lines of tomato for texture QTL and in assessing the structural variability and inheritance of hemicellulose structures in an apple progeny.[14,15]

Among fleshy fruits, peach and nectarine are economically important crops. Peaches are usually classified according to their melting, nonmelting, or stony-hard texture. Melting versus nonmelting is determined by a single gene located on chromosome 5, whereas the stony-hard trait is genetically independent from it.[16,17] The nature of peach cell wall polysaccharides, their modifications during fruit development, ripening, and texture elaboration have been the subject of several reports.[18−28] Peach cell wall polysaccharides are mainly composed of homogalacturonan (HG), rhamnogalacturonan I (RGI) rich pectin, and xyloglucan among the hemicellulose.[19,21] Homogalacturonan consists of a linear chain of α-1,4-linked D-galacturonic acids which can be partially esterified on O-6 by methanol and on O-2 or O-3 by acetic acid.

Received: April 10, 2012
Revised: June 13, 2012
Accepted: June 15, 2012
Published: June 15, 2012

Table 1. Structure and Nomenclature Used To Refer to Hemicelluloses and to Pectic Homogalacturonan Structures

Polysaccharides	Chemical structure	Code
Hemicelluloses	**Xyloglucan**	
	-β-D-Glc*p*-(1→4)	**G**[a]
	-β-D-Glc*p*-(1→4)- α-D-Xyl*p*-(1→6)↑	**X**
	-β-D-Glc*p*-(1→4)- β-D-Gal*p*-(1→2)-α-D-Xyl*p*-(1→6)↑	**L**
	-β-D-Glc*p*-(1→4)- α-L-Fuc*p*-(1→2)-β-D-Gal*p*-(1→2)-α-D-Xyl*p*-(1→6)↑	**F**
	Glucomannan	
	–β-D-Glc*p*-(1→4)-	**Hex**
	–β-D-Man*p*-(1→4)-	**Hex**
	Xylan	
	–β-D-Xyl*p*-(1→4)-	**Pen**
	α-D-GlcA*p*-(1→2)-	**u**
Pectin	**Homogalacturonan**	
	-α-D-GalA*p*-(1→4)-	**U**
	-4-deoxy-α-D-Gal-4-enosylA*p*-(1→4)-	**DU**
Substituting groups		
Methyl	CH_3-	**m**
Acetyl	CH_3-C(=O)-	**a**

[a]Elementary building block of xyloglucan structures:[43] **XLFG** is made of the linkage of **X**, **L**, **F**, and **G** elements. The number following **Hex**, **Pen**, **m**, or **a** refers to the number of these respective structures in the oligosaccharide.

Rhamnogalacturonan I is based on a backbone of alternating α-1,4-linked D-galacturonic acid and α-1,2-linked L-rhamnose residues. The latter sugar can bear side chains made of β-1,4-linked D-galactose, α-1,5-linked L-arabinose, or more complex combinations of arabinose and galactose residues.[29] Xyloglucans are based on a backbone made of 1→4 linked β-D-glucose residues mostly branched at O-6 by a α-D-xylosyl residue, which can be further extended by one β-D-galactosyl, by one β-D-galactosyl residue bearing one α-L-fucosyl residue, or by other combinations including α-L-arabinosyl residue.[30]

In this work the cell wall polysaccharide chemistry was characterized in commercial types of fruits and from the parents and offspring of specific crosses between two peach cultivars, Jalousia and Fantasia, and between Earlygold peach and Texas almond showing contrasted texture or morphological appearance. In particular, pectin-lyase and endoglucanase degradations of cell walls coupled to MALDI-TOF MS analysis of the products were proven useful to reveal genetically defined homogalacturonan and hemicellulose structures that are discussed with regard to quality traits and cell wall enzymes potentially affected between individuals.

MATERIALS AND METHODS

Peach Varieties and Hybrids. Fruits were from three groups of materials. A first group (A) was composed of four peach varieties with contrasted morphology and texture (three melting fruits, juicy nectarine "Zairegem − Royal Gem", pasty peach "Elegant Lady", and fibrous round peach "Maperla", and one nonmelting pavie peach "Coconut Ice"). These fruits were harvested at maturity in 2007 at INRA Bordeaux. A second group of fruits (B) was composed of individuals from crosses between Fantasia and Jalousia cultivars.[32] Besides the parents (Jalousia, flat peach; Fantasia, round peach), eight F2 progeny with contrasted phenotypes (F2#25, round peach; F2#31, flat peach; F2#71, round nectarine; F2#74, round peach; F2#82, round nectarine; F2#143, round peach; F2#178, flat peach; F2#210, round peach) were harvested at maturity in 2009 at INRA-Bordeaux. The third group of fruits (C) consisted of a collection of individuals from crosses between peach (Earlygold) and almond (Texas).[16] Besides the parents and their F1 hybrid (TxE_F1), three F2 (F2#17, peach-like; F2#23, almond-like; F2#94, hybrid-like) and two backcross (BC1#9, juicy; BC1#78, nonjuicy) progeny were harvested at maturity in 2009 at IRTA-Barcelona. For all groups, the flesh of 3 to 5 fruits per genotype was cut into about 1−2 cm^3 pieces and immediately frozen at −80 °C.

Cell Wall Preparation. The frozen flesh samples from three to five fruits per genotype were freeze-dried. Each dried sample was ground to a fine powder (FastPrep, MP Biomedicals, Solon, OH, USA) and extracted with 80% ethanol at 85 °C and 35 bar in an automated solvent extractor (ASE200, Dionex Sunnyvale, CA, USA) until the

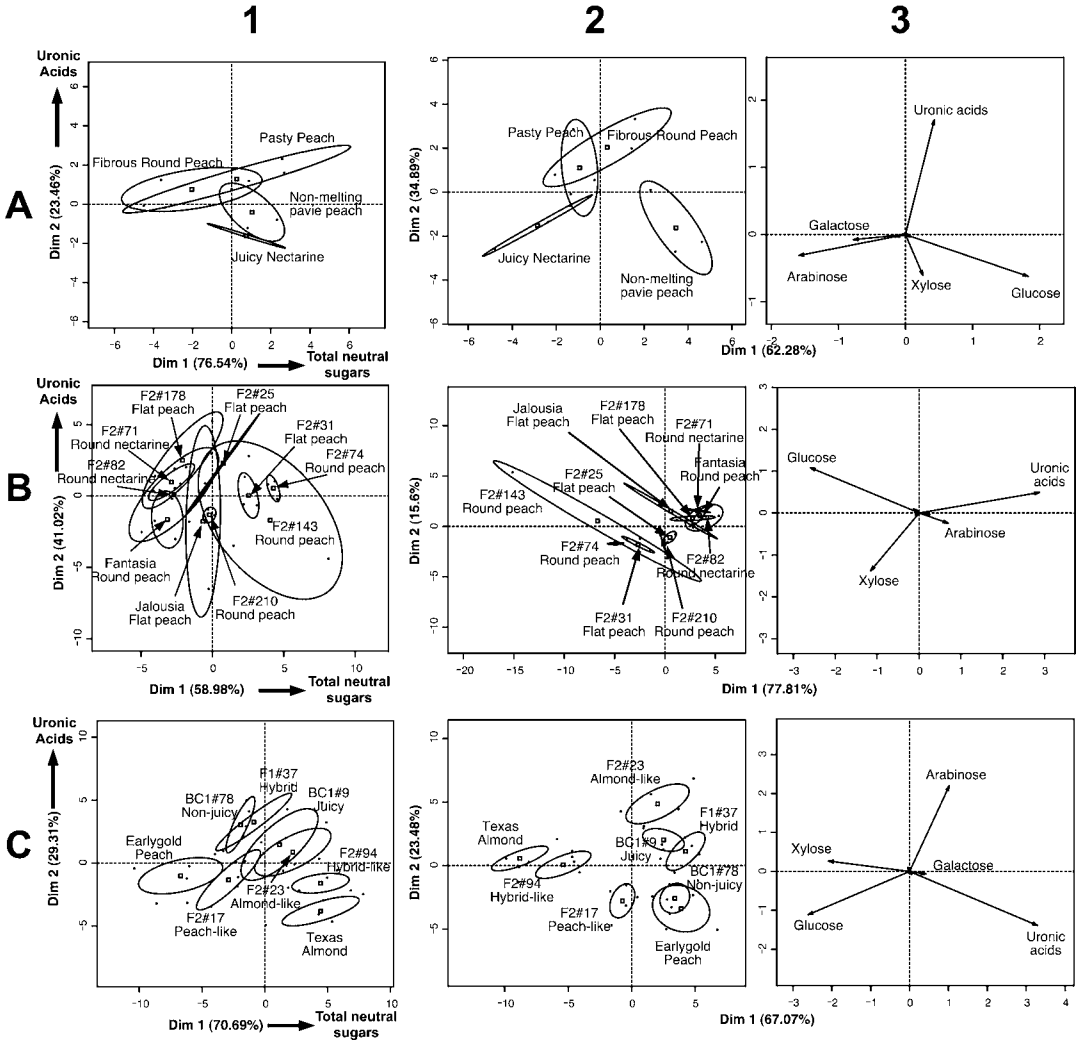

Figure 1. PCA analysis of sugar composition in the cell wall preparations from peach with contrasted texture (A), from the Jalousia × Fantasia cross (B), and from the Texas almond and Earlygold peach cross (C). (1) Neutral sugar and uronic acid content on the dry weight basis, (2 and 3) sugar composition on the molar percentage basis: (2) individual and (3) variable maps. Minor contributions of sugars are not indicated on the variable map. Ellipses correspond to 95% confidence region of individuals.

ethanol solution was free of soluble sugars. The alcohol insoluble material (AIM) was dehydrated at 40 °C under vacuum over P_2O_5. All biochemical measurements were performed from dry AIM.

Cell Wall Sugar Composition. Identification and quantification of cell wall neutral sugars were performed by gas−liquid chromatography (GC) after sulfuric acid hydrolysis.[33] AIM was dispersed in 13 M sulfuric acid for 30 min at 30 °C and then hydrolyzed in 1 M sulfuric acid (2 h, 100 °C). Sugars were converted to alditol acetates and chromatographed on a DB 225 capillary column (J&W Scientific, Folsorn, CA, USA; temperature 205 °C, carrier gas H_2).[34] A standard sugar solution and inositol as internal standard were used for calibration. Uronic acids in acid hydrolysates were quantified using the metahydroxydiphenyl colorimetric acid method.[35]

Cell Wall Polysaccharide Enzymatic Profiling. Cell wall material (5 mg) from each fruit per genotype was suspended in 1 mL of acetate buffer (5 mM, pH 5) or water and degraded by pectin lyase prepared according to Ralet et al.[36] (0.55 nkatal) or by commercial endo-1,4-β-glucanase from *Trichoderma longibrachiatum* (Megazyme, Bray, Ireland; 20 U), respectively. After overnight digestion at 40 °C under head-over-tail mixing, the suspension was centrifuged (10 min, 14000*g*) and the supernatant solution was heated for 10 min in a boiling water-bath to inactivate enzymes. Oligosaccharides in the hydrolysates were analyzed by MALDI-TOF MS in the positive mode using an Autoflex III MALDI-TOF/TOF spectrometer (Bruker Daltonics, Bremen, Germany) equipped with a Smartbeam laser (355 nm, 200 Hz). Two types of matrix were used for enzyme hydrolysate analysis. For pectin-lyase hydrolysates, the ionic liquid matrix DMA/DHB was prepared and used as reported.[37] Calibration was realized with galactomanno-oligosaccharides (DP 3 to 9) of known masses. The glucanase hydrolysates were analyzed using the Super DHB matrix.[38] The matrix was prepared by a mixture (90/10, v/v) of 2,5-dihydroxybenzoic acid (DHB) at 10 mg/mL in water and 2-hydroxy-5-methoxybenzoic acid at 10 mg/mL in pure methanol, respectively. The instrument was externally calibrated using the monoisotopic masses of main oligosaccharides ($[M + Na]^+$ ion) released from xyloglucans (**XXG**, 791.243 Da; **XXXG**, 1085.338 Da; **XXFGa1**, 1435.459 Da; **XLFGa1**, 1597.512 Da; see below for nomenclature).

Spectra were recorded in the mass range *m*/*z* 600−1400 and 700−1700 for the pectin-lyase and glucanase hydrolysates, respectively. Spectra were exported to Flex Analysis 3.0 software (Bruker) and preprocessed. Mass lists reporting *m*/*z* (monoisotopic masses, after deisotoping with the SNAP algorithm, Bruker) and intensities of detected ions were then exported for statistical analysis and graphical representation. Ion masses and intensities on the pectin-lyase spectra were normalized according to the ion peak at *m*/*z* 783.191 attributed to **DU4m4** (see below for nomenclature). Ion masses and intensities on the glucanase spectra were normalized to that of the **XXXG** ion.

Identification of ions was done by comparison with the m/z lists registered (± 0.2 m/z) to theoretical masses of the sodium adduct of different oligosaccharides.

For oligouronides released by pectin-lyase, this list took into account specificities of the enzyme.[36] In particular, because several oligosaccharide structures have similar m/z values due to substitutions by methyl and acetyl esters and by different ion adduct types (sodium or potassium) combined with various salt forms (Na-H) on acidic functions, ion identification was performed according to a minimum methyl esterification per oligosaccharide (i.e., DP3, 1 to 3 methyl esters; DP4, 2 to 4; DP5, 2 to 5; DP6, 3 to 6; and DP7, 4 to 6) and a maximum of 1 to 2 acetyl groups depending on degree of polymerization (DP3 to 5, 1 acetyl; DP 6 and 7, 2 acetyl groups).

For oligomers released by the commercial glucanase, ion attribution was realized based on combinations of hexoses, methyl-pentoses, pentoses, and acetyl ester substituents. The enzyme preparation is known to hydrolyze glucomannan and to contain minor xylanase and galactanase contaminating activities.[14] Xyloglucan structures were ions of mass corresponding to combinations of hexose and pentose with methyl-pentose and/or acetyl ester substituents. Ions of m/z corresponding to combinations of hexoses and acetyl ester substituents were attributed to glucomannan structures. Ions of mass corresponding to pentose and combinations of pentose and uronic acid were attributed to xylan.

Oligosaccharide nomenclature was as follows. For polyuronides the letter **U** corresponds to uronic acid. The following number refers to the number of residues in the oligomer (i.e., DP). Acetyl and methyl esters substitutions were referred to as **a** and **m**, respectively, followed by the amount of groups. The unsaturation of the uronic acid at the nonreducing end of the oligomer released by pectin-lyase was referred to as **D**. Other adducts of oligouronides were referred to as **Na-H** and **K**. According to this nomenclature, **DU4m4** refers to an oligohexouronide of DP4 fully methyl esterified and unsaturated at the nonreducing end.

The nomenclature of oligomers released by glucanase followed that established for xyloglucans extended to account for acetyl groups noted **a** (Table 1).[30] Hexose containing oligosaccharides attributed to glucomannans were noted **Hex** extended by the letter **a** for acetyl esterification. The number following the structure codes denotes the number of building structures and acetyl groups in the oligosaccharides (i.e., **Hex3a2** corresponds to 3 hexosyl units and 2 acetyl groups).

Statistical Analysis. Data treatments and statistical analyses were performed with R software.[39] Exploratory statistics consisted of principal component analysis of the chemical data and MALDI-TOF MS ion intensities. Significant differences between individuals were evaluated by a Student test performed on PCA individual coordinates on principal components. Significant differences were set at a probability value of equality below 5%. Pearson correlation coefficients were computed within MALDI-TOF MS ion data sets.

RESULTS

The Peach Cell Wall Sugar Composition Varies between Peach Genotypes. Cell wall polysaccharides from the different genotypes are made of glucose, galactose, arabinose, xylose, rhamnose, fucose, mannose, and uronic acids (Supplementary Table 1 in the Supporting Information) as already reported in peaches.[20,24,26,31] Variations in total neutral sugars and uronic acids on the cell wall material dry weight basis and individual sugars on the molar percentage basis were assessed by principal component analysis (PCA; Figure 1) by groups of peach genotypes. These groups were composed of contrasted texture varieties (Figure 1 A), individuals from the cross between Jalousia and Fantasia peaches (Figure 1 B), and individuals from the cross between the Earlygold peach and Texas almond (Figure 1 C). Variations in total neutral sugars and uronic acids were mainly accounted for by principal components 1 and 2, respectively (Figure 1-1). The contribution of the different sugars to the dispersion of individuals on the PCA maps (Figure 1-2) is shown in Figure 1-3.

Among the contrasted texture peach varieties "juicy nectarine" differed from "pasty peach" with a low uronic acid content (Figure 1 A1; Supplementary Table 2a in the Supporting Information). Individuals from the Jalousia × Fantasia crosses differed on their total neutral sugar content (Figure 1B1; Supplementary Table 2b in the Supporting Information). The low neutral sugar content in the parent Fantasia significantly differed from F2#31 and F2#74 as well as F2#143. Other significant differences were noted between F2#31 and F2#71 as well as F2#82, between F2#71 and F2#74 as well as F2#143, between F2#74 and F2#82 as well as F2#178, between F2#82 and F2#143, and between F2#143 and F2#178. The cross between Earlygold peach and the Texas almond gave rise to more contrasted individuals (Figure 1 C1; Supplementary Table 2c in the Supporting Information). On the neutral sugar content basis, the genotype BC1#78 differed significantly from F2#94 and Texas while F2#17 differed from F2#94 and Texas. The parent Earlygold with a low content in neutral sugars differed from all genotypes except BC1#78 and F2#17. On the uronic acid content basis, F1#37 differed significantly from all other genotypes except BC1#78, BC1#9, and F2#23. Texas also differed from all other individuals except Earlygold, F2#17, and F2#94. Other significant differences were noted between BC1#78 and the three genotypes: Earlygold, F2#17, F2#94.

With regard to individual sugars, significant differences were noted between nonmelting pavie peach and juicy nectarine and pasty peach according to the first component. The latter opposed glucose to arabinose contents (Figure 1A2,A3). The nonmelting pavie peach was significantly richer in glucose compared to the pasty and juicy peaches (Supplementary Table 3a in the Supporting Information). Individuals from the cross between Fantasia and Jalousia differed from one another along the first component, which reflected essentially variations in glucose and uronic acid proportions (Figure 1B2,B3). Significant differences were noted between Fantasia and F2#74 as well as F2#143, between F2#71 and F2#143, between F2#74 and F2#82, between F2#82 and F2#143, and between F2#143 and F2#178 (Supplementary Table 3b in the Supporting Information). Again, the cross between Earlygold and Texas yielded individual genotypes with remarkable composition differences according to the two first principal components (Figure 1C2,C3). The first axis reflected essentially variations in xylose and glucose contents that were opposed to that of uronic acid while variation in arabinose proportion was the main contributor to the second axis. According to the first PCA axis, the parent Texas and F2#94, with a higher proportion of xylose and glucose, were close and significantly different from all other genotypes (Supplementary Table 3c in the Supporting Information). F2#17 differed significantly from the four genotyptes: BC1#78, F1#37, F2#94, and Earlygold. On the second axis, F2#23 differed significantly from all other genotypes with regard to a high arabinose proportion. In contrast, Earlygold differed significantly from all other genotypes except BC1#78 and F2#17. F2#17 differed from all other genotypes except BC1#78 and Earlygold. Other significant differences were noted between BC1#78 and the three genotypes: BC1#9, F1#37, Texas.

Peach Genotypes Can Be Distinguished According to the Fine Structure of Their Cell Wall Pectin. In order to assess variations in the fine structure of the homogalacturonan

regions in pectins, cell walls were subjected to pectin lyase hydrolysis and oligosaccharides produced were analyzed by MALDI-TOF MS. A typical MALDI-TOF MS spectrum is shown in Figure 2. Major ions correspond to the series of

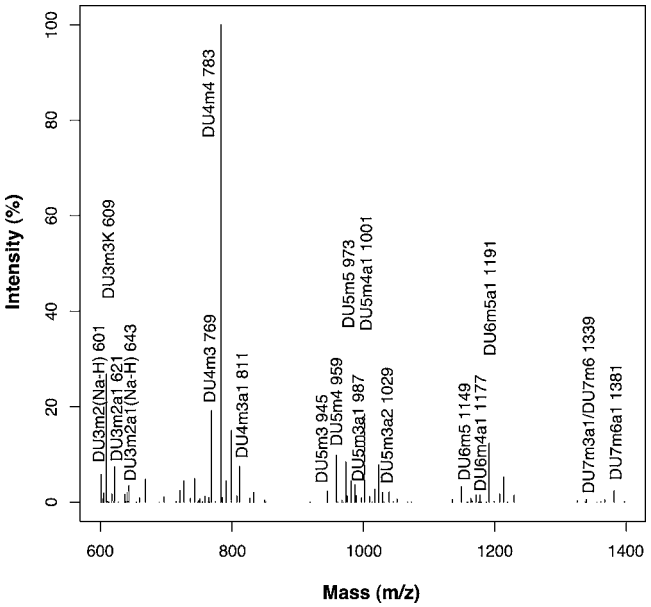

Figure 2. Mean MALDI-TOF MS spectrum of pectin lyase hydrolysate of peach/almond cell walls. Only ions in their sodium adduct form are depicted except for oligomers of DP3 (**DU3m2**). Nomenclature of the ions is as described in the text.

oligouronides of degree of polymerization (DP) 4 with minor ions of DP2, 3, 5, 6 and traces of DP7. Among these DPs, different methyl and acetyl esterification forms were observed.

Variations in the proportion of the different oligouronides within the different groups of fruits were assessed by PCA (Figures 3−5). Among the contrasted commercial type of peach varieties, individuals were distinguished on the first two components according to contributions of **DU3m3K**, **DU4m4K**, **DU6m5a1**, **DU5m4a1**, and **DU5m4** oligomer intensities (Figure 3). The juicy nectarine with higher proportions of **DU3m3K** was significantly different from the other varieties (Supplementary Table 4a in the Supporting Information). On the second axis, the fibrous peach significantly differed from the other varieties due to contributions of **DU6m5a1** and **DU5m4a1** and a lower contribution of **DU3m3K** and **DU5m4**.

Individuals from the Jalousia × Fantasia peach cross were distinguished mainly according to the intensity of **DU3m3K** and **DU4m4K** ions on the first component (Figure 4). F2#82 significantly differed from all other individuals except F2#143 and F2#210 (Supplementary Table 4b in the Supporting Information). F2#143 also differed from all other genotypes except F2#25, F2#143, F178, and Jalousia. F2#210 also differed from all others with the exception of F2#25, F2#82, and F2#143. Additional significant differences were noted between Jalousia and F2#31, between Fantasia and F2#25, and between F2#25 and F2#31. The second component distinguished individuals mainly on the intensity variations of **DU6m5a1** and **DU5m4a1** ions. Significant differences were noted between F2#74 and the three genotypes: F2#82, F2#178, and Jalousia, between Fantasia and F2#178 as well as Jalousia, and between F2#143 and F2#178 as well as Jalousia. Taking the different morphologies into account, flat fruits differed significantly from round fruits on the second component (ANOVA p value = 0.0009 according to PC2). Round fruits were characterized by a greater contribution of fully methylated oligouronides while partially methylated and acetylated oliguronides characterized flat fruits.

Within individuals from the cross between Earlygold peach and Texas almond (Figure 5), the almond parent with a high contribution of **DU3m3K** ion intensity differed significantly on the first component from all other genotypes. On this axis, the almond-like F2#23 individual also significantly differed from BC1#78 and F2#17 (Supplementary Table 4c in the Supporting Information). The second component clearly distinguished BC1#78 from F2#94 as well as Texas, between BC1#9 and F2#23, between Earlygold and the three genoytpes: F2#17, F2#94, and Texas, between F1#37 and Texas, between F2#17 and F2#23, between F2#94 and F2#23, and between F2#23 and Texas mainly on the variable contribution of **DU6m5a1** and **DU5m4a1** ion intensities. The third principal

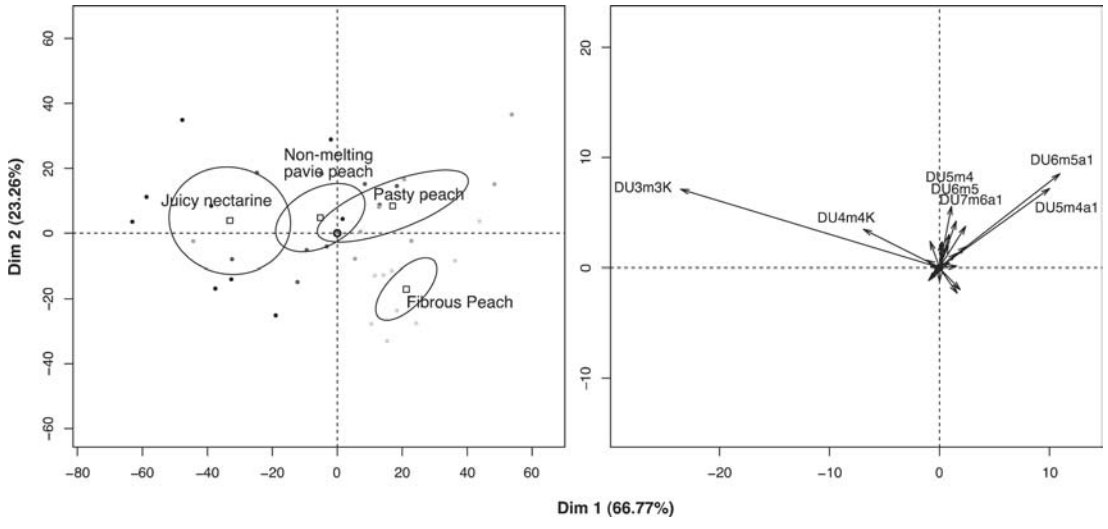

Figure 3. PCA analysis of MALDI-TOF MS spectra from the pectin-lyase hydrolysate of cell wall preparations from texture contrasted peach. Left: individual map. Right: variable map. Nomenclature as described in the text. Ellipses correspond to 95% confidence region of individuals.

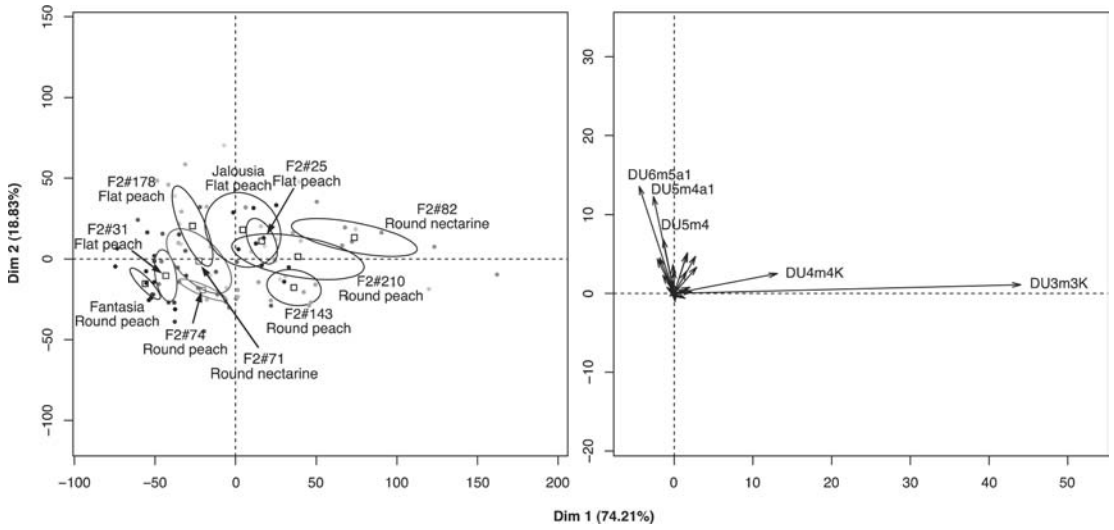

Figure 4. PCA analysis of MALDI-TOF MS spectra from the pectin-lyase hydrolysate of cell wall preparations from Jalousia × Fantasia cross. Left: individual map. Right: variable map. Nomenclature as described in the text. Ellipses correspond to 95% confidence region of individuals.

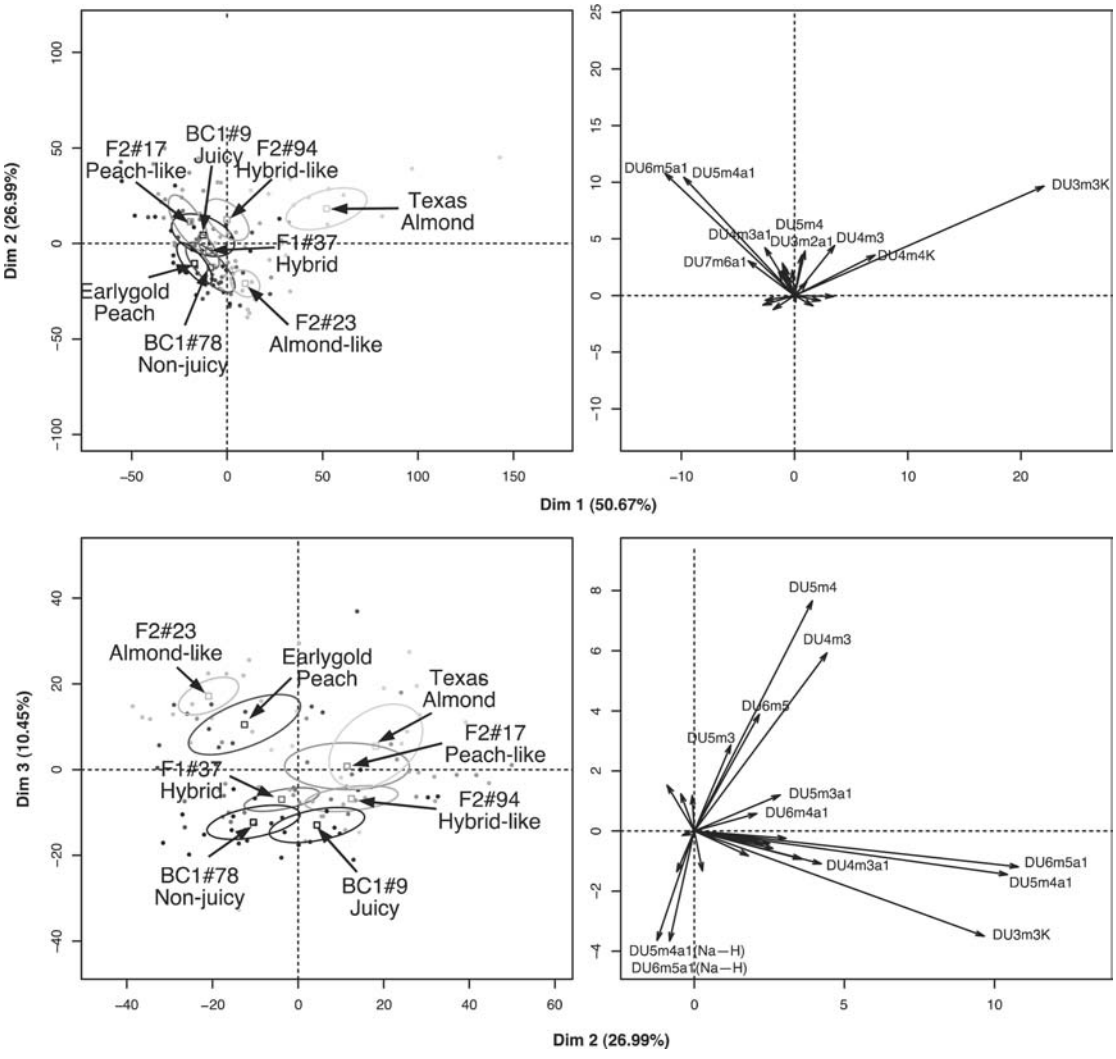

Figure 5. PCA analysis of MALDI-TOF MS spectra from the pectin-lyase hydrolysate of cell wall preparations from Earlygold peach × Texas almond. Left: individual map. Right: variable map. Top: components 1 and 2. Bottom: components 2 and 3. Nomenclature as described in the text. Ellipses correspond to 95% confidence region of individuals.

dx.doi.org/10.1021/jf301494j | J. Agric. Food Chem. 2012, 60, 6594−6605

Table 2. Correlation between Oligouronides Ion Intensity (X, Y) within the Three Groups of Fruits: Contrasted Peach Varieties (A), Fantasia and Jalousia Peaches and Genotypes from their Cross (B), and Earlygold Peach and Texas Almond and Genotypes from their Cross (C)

X	Y	A	B	C	X	Y	A	B	C	X	Y	A	B	C
DU3m2(Na-H)	DU4m3(Na-H)	0.73	0.71	0.85	DU4m4K	DU5m5K	0.89	0.91		DU5m5K	DU5m4a1K		0.71	
	DU5m4(Na-H)			0.76		DU5m4a1(Na-H)K		0.8			DU5m4a1(Na-H)K		0.8	
											DU6m5a1(Na-H)K		0.72	
DU3m2(Na-H)	DU4m3a1	−0.79			DU4m3a1	DU5m3a1	0.84	0.86	0.77					
	DU5m4a1	−0.81				DU5m4a1	0.94	0.86	0.82	DU5m4a1	DU5m4a1K		0.7	
	DU6m5a1	−0.82				DU5m4(Na-H)	−0.7				DU6m4a1			0.82
	DU6m5a1K	−0.7				DU5m4a1K		0.7	0.74		DU6m5a1	0.99	0.97	0.97
						DU5m3a2			0.81		DU6m5a1K		0.8	0.82
DU3m3K	DU4m4K	0.95	0.94	0.96		DU6m4a1			0.73		DU7m6a1		0.85	0.93
	DU5m5			−0.74		DU6m5a1	0.93	0.78	0.74					
	DU5m5K	0.85	0.82			DU6m5a1K		0.72	0.78					
	DU5m4a1(Na-H)K		0.76			DU7m6a1			0.7	DU5m4a1K	DU6m5	0.74		
											DU6m5a1K	0.97	0.95	0.88
DU3m2a1(Na-H)	DU5m4a1(Na-H)			0.7	DU5m3	DU5m4		0.83	0.83		DU7m3a1	0.76		
						DU6m5		0.74	0.71					
DU3m2a1	DU4m3a1		0.74			DU7m3a1		0.72		DU5m4a1(Na-H)	DU6m5a1(Na-H)		0.87	0.92
	DU5m3a1		0.72								DU6m5a1(Na-H)	0.95		
	DU5m4a1K		0.72		DU5m4	DU5m4K	0.83							
						DU6m5	0.94	0.93	0.87					
DU3m2a1(Na-H)	DU5m4	−0.74				DU5m4a1(Na-H)			−0.72	DU5m4a1(Na-H)K	DU6m5a1(Na-H)K		0.89	
	DU6m5	−0.77				DU7m3a1	0.91	0.87						
	DU7m3a1	−0.75								DU6m5	DU7m3a1		0.9	
					DU5m4K	DU5m4a1K		0.79						
DU4m3	DU5m3		0.74	0.9		DU6m5a1K		0.72		DU6m4a1	DU6m5a1			0.81
	DU5m4	0.93	0.79	0.83		DU6m5	0.75				DU6m5a1K			0.72
	DU5m4K	0.78	0.82			DU7m3a1	0.75				DU7m6a1			0.76
	DU5m3a1		0.74			DU5m4a1(Na-H)	−0.75							
										DU6m5	DU6m5a1K	0.72	0.76	0.77
DU4m3	DU6m5	0.86			DU5m4(Na-H)	DU6m5(Na-H)	0.83				DU7m3a1	0.97		
	DU7m3a1	0.81				DU5m4a1	−0.7							
						DU6m5a1	−0.72			DU6m5a1	DU7m6a1		0.9	0.96
DU4m3(Na-H)	DU5m4(Na-H)	0.84		0.81										
	DU4m3a1	−0.72			DU5m3a1	DU5m4a1	0.88	0.83	0.71	DU6m5a1K	DU7m3a1	0.74		
	DU5m4a1	−0.73				DU5m4a1K		0.72	0.72		DU7m6a1			0.7
	DU6m5a1	−0.74				DU6m5	0.7							
						DU6m5a1	0.86	0.74	0.83					
						DU6m5a1K		0.73	0.74					
						DU7m3a1	0.75							

dx.doi.org/10.1021/jf301494j | J. Agric. Food Chem. 2012, 60, 6594−6605

component explaining 10.5% of the total variance distinguished further individuals (Figure 5). It mainly accounted for variations in the intensity of **DU5m4**, **DU4m3**, **DU6m5**, **DU5m3**, **DU5m4a1(Na-H)**, and **DU6m5a1(Na-H)** ions. In particular F2#23 significantly differed from all other individuals except Earlygold. On the contrary, BC1#9 and BC1#78 differed from one another and from all other individuals except F1#37 and F2#94. Additional significant differences were noted between Earlygold and the four genotypes F1#37, F2#94, F1#37, and Texas and between F2#94 and Texas.

In order to search for relationships between homoglacturonan methyl and/or acetyl esterification features within peach genotype groups, Pearson correlation coefficients were calculated between oligomers' MALDI-TOF ion intensity ($r \geq 0.7$; Table 2). There were no or rare correlations between monosodium adducts of partially methylated oligomers and the salt form of the corresponding adduct (Na-H on the free carboxylic acid) or between sodium and the potassium oligomer adducts. These reflected unclear complex ionization mechanisms of oligouronides in DMA/DHB matrix. There were strong correlations between several structures observed in the three groups of fruits: **DU3m2(Na-H)/DU4m3(Na-H)**, **DU3m3K/DU4m4K**, **DU4m3/DU5m4**, **DU4m3a1/DU5m3a1/DU5m4a1/DU6m5a1**, **DU5m4/DU6m5**, **DU5m4a1K/DU6m5a1K**, and **DU6m5/DU6m5a1K**. These correlations testified structural similarities across the three groups of fruits and affiliations of oligomers resulting from close demethyl esterification mechanisms of pectin in cell walls. Other correlations concerned two or only one group of samples. These reflected genotype specific demethyl esterification and/or acetyl esterification of pectin.

The Fine Structure of Hemicellulose in Peach Cell Wall Varies with Genotypes. The cell wall polysaccharides in the peach collections were hydrolyzed by an endoglucanase to assess the fine structure variability of hemicelluloses. A typical MALDI-TOF MS spectrum of the hydrolysis products (Figure 6) showed major ions with m/z corresponding to

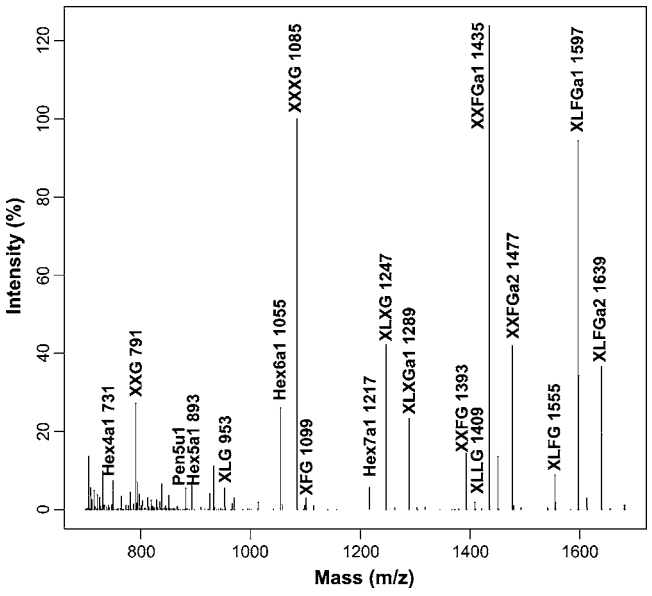

Figure 6. Mean MALDI-TOF MS spectrum of glucanase hydrolysate of peach/almond cell walls. The nomenclature is as described in the text.

XXFGa1, **XLFGa1**, and **XXXG** xyloglucan structures. Lower intensity ions correspond to **XLXG**, **XXFGa2**, and **XLFGa2** xyloglucan structures and glucomannan oligomers (**Hex6a1**). Other small ions were attributed to xyloglucan and glucomannans as well as minor contribution of xylan substituted by uronic acid (**Pen5u1**). Structural variation in the glucanase hydrolysates of the different fruit groups was assessed by PCA (Figures 7−9).

Texture contrasted peach varieties of commercial type were distinguished from one another according to the second component (Figure 7) which opposed primarily **XLXGa1**, **XXG** to **XLFG**, **XXFG** ion intensity variations. The four varieties differed significantly from one another along this axis (Supplementary Table 5a in the Supporting Information), the pasty peach being the richest in **XLXGa1** and the juicy nectarine the richest in **XXFG** and **XLFG** structures, which are highly correlated.

The glucanase hydrolysate profile allowed a limited discrimination among individuals from the cross between Jalousia × Fantasia peaches on the first two principal components (Figure 8). These two axes accounted for monoacetylated **XLFGA1**, **XXFGa1**, and diacetylated **XLFGa2**, **XXFGa2** ion intensity variations, which are highly correlated, respectively. Component 2 opposed contributions of primarily **XLFG**, **XXFG** to that of **XLFGa2**, **XXFGa2** ion intensity. On the first axis, F2#178 significantly differed from the four genotypes: Fantasia, F2#31, F2#71, and F2#74, and F2#82 differed significantly from F2#31 and F2#71 (Supplementary Table 5b in the Supporting Information). On the second axis, Jalousia significantly differed from F2#82 and F2#210, and Fantasia differed significantly from F2#25, F2#31, F2#82, and F2#210. The third principal component furthered the differentiation of individuals primarily on the basis of the variation in the ion intensity of **XLFGa1** opposed to **XLXFGa1**, **XXFGa1**, **XXG**, and **XLFGa1** xyloglucan structures. Jalousia differed significantly from all other genotypes along this axis. F2#71 also differed from most other individuals except F2#178. F2#210 significantly differed from most other individuals except Fantasia, F2#31, F2#74, and F2#143. Additional significant differences were noted between Fantasia and F2#178, F2#25 and F2#74, and F2#31 and F2#178, as well as between F2#74 and F2#178.

Genotypes from the cross between Texas almond and Earlygold peach presented remarkable different glucanase profiles that allowed a clear distinction of nearly all genotypes on the first principal component (Figure 9). This first axis mainly opposed **XLFGa2**, **XLFG** to **XXFGa1** ion intensity variations. All genotypes significantly differed according to this axis except Earlygold, F2#17, and F2#94 and between F2#17 and F2#94 (Supplementary Table 5c in the Supporting Information). The second axis essentially accounting for **XLFGa1** ion intensity variation distinguished Texas from all other genotypes except F2#94. F2#17 also significantly differed from F2#94.

Few MALDI-TOF ion intensities of xyloglucan and glucomannan oligomers correlated with each other (Table 3). Common correlations between **XLFGa1** and **XLFGa2** were only observed for contrasted commercial type varieties and for genotypes from the Jalousia × Fantasia peach cross.

DISCUSSION

Peach and nectarine cell wall polysaccharides composition are affected by genetic factors.[24,25,28,31] Accordingly, significant

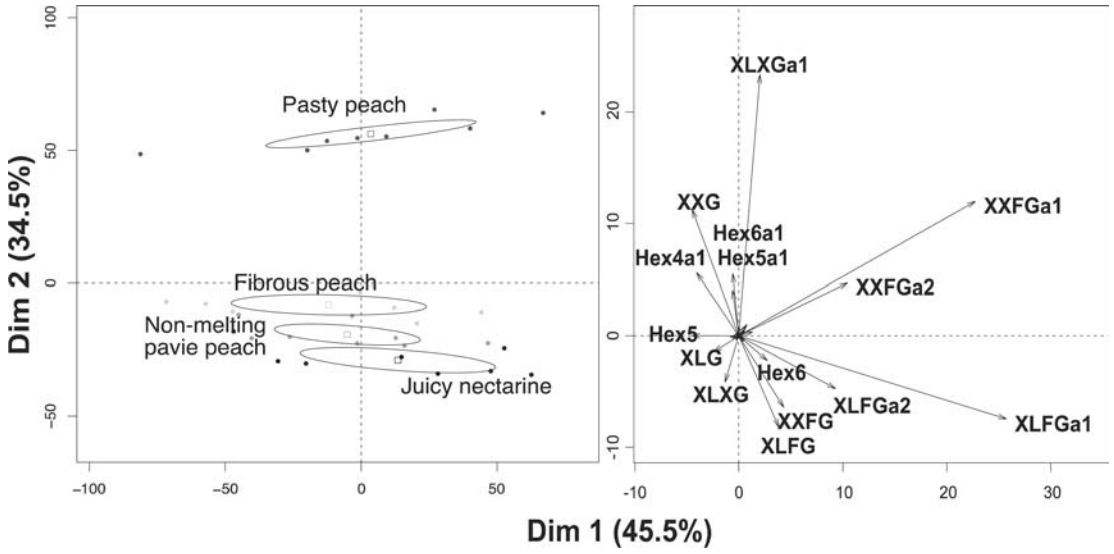

Figure 7. PCA analysis of MALDI-TOF MS spectra from the glucanase hydrolysate of cell wall preparations from texture contrasted peach. Left: individual map. Right: variable map. Nomenclature as described in the text. Ellipses correspond to 95% confidence region of individuals.

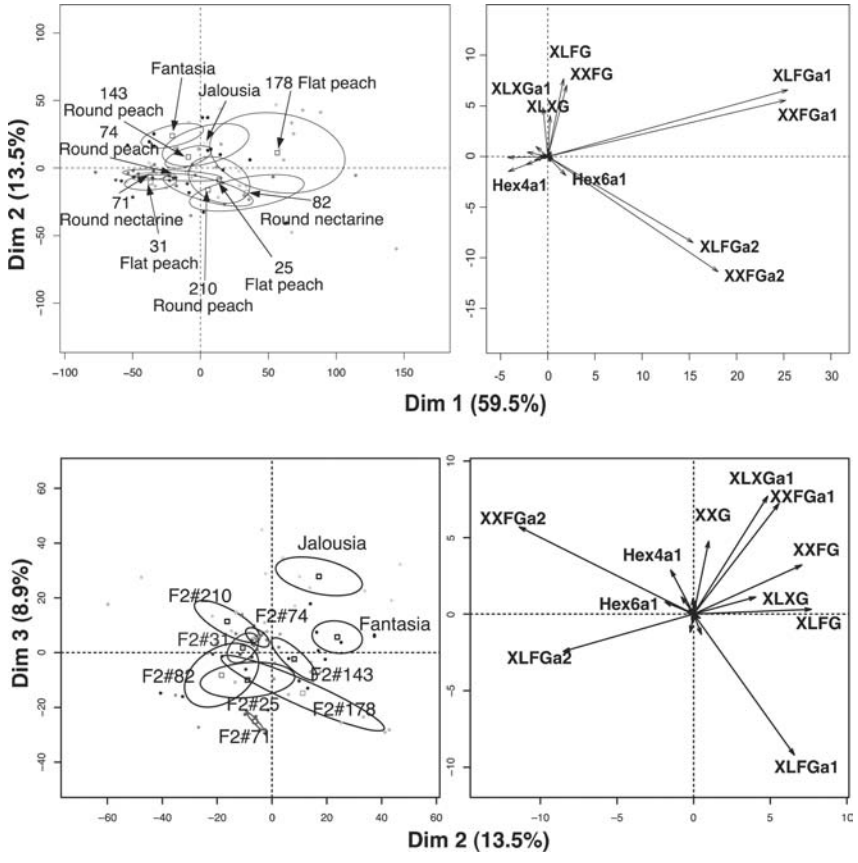

Figure 8. PCA analysis of MALDI-TOF MS spectra from the glucanase hydrolysate of cell wall preparations from the Jalousia × Fantasia cross. Left: individual map. Right: variable map. Top: components 1 and 2. Bottom: components 2 and 3. Nomenclature as described in the text. Ellipses correspond to 95% confidence region of individuals.

variations of uronic acids and total neutral sugar composition on the weight basis of the cell wall material were observed between the different individuals from the three groups of fruit in the present study. They reflected variable contents in pectins (mainly HG), other matrix glycans (RGI-rich pectins and hemicellulose), and cellulose as well as nonsugar components (i.e., proteins). This composition discriminated particularly the different genotypes from the cross of Texas almond and Earlygold peach parents with contrasted fruit traits. The progenies were grouped between their parents, some in close proximity of which they shared the overall fruit traits. The cell wall sugar representative of the main cell wall polysaccharides discriminated better the different individuals in the three groups of genotypes. Uronic acids (pectin) and glucose and xylose

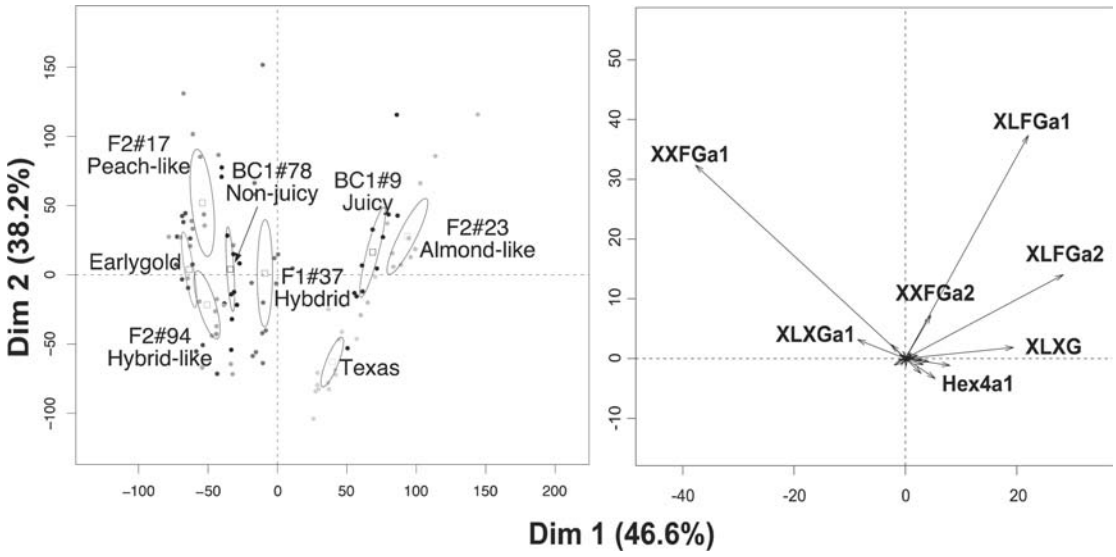

Figure 9. PCA analysis of MALDI-TOF MS spectra from the Texas almond and Earlygold peach cross. Left: individual map. Right: variable map. Nomenclature as described in the text. Ellipses correspond to 95% confidence region of individuals.

Table 3. Correlation between Glucanase MALDI-TOF MS Ion Intensity (X, Y) within the Three Groups of Fruits: Contrasted Peach Varieties (A), Fantasia and Jalousia Peaches and Genotypes from their Cross (B), and Earlygold Peach and Texas Almond and Genotypes from their Cross (C)

X	Y	A	B	C
XLFG	XXFG		0.82	
XLFGa1	XLFGa2	0.77	0.72	
XLLG	Hex5a2			0.75
XLXGa1	XXG	0.82		
XLXGa1	Hex6a1	0.76		
XXFG	XLFG	0.89		
XXFGa1	XXFGa2	0.88		
XXFGa1	XLXGa1			0.74
XXFGa1	XLFGa1		0.77	
XLXG	XLFGa2			0.73
XLXG	XLLG			0.71
XLXGa1	XLFG	−0.72		
XXFGa2	XLFGa2		0.9	
XXG	Hex6a1	0.74		
XXG	XLFG	−0.72		
Hex6a1	Hex7a1			0.73

(cellulose/xyloglucan) proportions were the main discriminants between the genotypes and to a variable extent, arabinose and galactose attributed essentially to rhamnogalacturonan I pectin side chains. Sugar composition may help distinguishing cell wall contributors to contrasted fruit traits such as galactose and arabinose often associated with mealiness and wooliness textures in peach.[21,27] In the present case, xylose and/or glucose rich cell walls from almond and hybrid-like phenotype or from nonmelting pavie peach were distinguished from other genotypes though the relation between these high sugar proportions with fruit shape or texture remains to be established. In fact sugar composition was not able to distinguish fruits with different shapes from the Fantasia × Jalousia peach cross.

Peach meltiness and stony-hard textures have been related to homogalacturonan pectin structure while fruit softening implies hemicellulose structural changes with yet unclear implications of its fine structure.[19,20,24,25,40,41] More detailed structural cell wall polysaccharide analysis was realized to provide clues on which sets of enzymes may contribute to cell wall reshuffling in texture elaboration and fruit shape development.

Homogalacturonan (HG) pectin methyl esterification is known to impact cell−cell adhesion and to regulate endopolygalacturonase degradation with implications on fruit texture and plant organ morphogenesis.[42,43] Less documented, acetyl esterification of pectin is known to perturb HG calcium mediated dimerization in vitro, which may potentially affect cell−cell adhesion in vivo.[44] Although the fruit ripening stage can affect the HG methyl esterification, clear differences were observed between the different genotypes according to the proportion of highly methylated oligomers and partially methyl- and acetyl-esterified ones. Correlations between the MS peak intensities of fully methyl-esterified or partially methyl- and acetyl-esterified oligomers across the three different groups of fruits indicate similar processing mechanisms of methyl-ester removal from the native highly esterified pectin by pectin methyl-esterases (PME).[29] In contrast correlations limited to specific groups highlight genetically controlled PME activities. Of interest is the relationship between fruit shape and the proportion of partially methyl and acetyl-esterified oligomers. Fruit shape may involve specific HG biosynthesis and pectin methyl- and/or acetyl-esterase remodeling during organ development. Pectin methyl esterification modulation by PME has already been shown to affect hypocotyl or stem growth.[45,46]

Xyloglucan plays a key role on fruit texture.[47] Fruit ripening upregulates the hemicellulose structural reshuffling by xyloglucan endotransglusosylase/hydrolases (XET/XTH) as well as the loosening of its interactions with cellulose by expansin. Its fine structure is known to vary with genetics, with organ development and fruit ripening.[12,14,15,48] The present results show that its fine structure is also affected by genetics in peach. In fact, variations in the xyloglucan fine structure discriminated better the different genotypes in the three peach groups than pectin lyase hydrolysis did. The least discriminated genotypes were from the Jalousia and Fantasia peach cross.

Morphological traits do not appear to involve specific xyloglucan structural features. The low level of correlation between structural variations shared by the three groups of fruits indicates a tight genetic regulation of biosynthesis and/or remodeling of peach xyloglucan. Structural variations impacted side chain sugars and acetyl-esterification and may involve specific osidases.[49] The relation between xyloglucan fine structure, cellulose interactions, cell wall mechanical properties, and fruit texture remains to be established. Galactosylation of xyloglucan side chains appears to play a role in cell wall mechanical properties.[50] It may be important in regulating XET/XTH activities.[51]

With regard to the impact of genetics on cell wall chemistry, a strong correlation is apparent between genetic distance of the individuals sampled and variability for all cell wall polysaccharide characters studied here. In the parents and offspring of the most distant progenies (almond × peach) results obtained were clearly contrasted and parents and progeny were often distinguishable among them and with the parents. On the other hand, the two parents of the peach F2, Jalousia and Fantasia, while differing in various morphological characters of simple inheritance, were genetically close. Differences in cell wall polysaccharides among them and in their offspring were slighter but showed significant differences of methyl esterification of pectins related with their flat or round fruit morphology. The four peach cultivars with contrasted fruit features were of different origins and of an intermediate level of genetic diversity as corroborated with the chemical data.

In conclusion, the variation of cell wall polysaccharide composition and structure in peaches and related genotypes with contrasted texture and morphological traits is conveniently shown by chemical means and enzymatic degradation by pectin lyase and glucanase coupled to MALDI-TOF MS. The results indicate that pectin methyl- and acetyl-esterification appear associated with fruit shape and that xyloglucan fine structure is under a fine genetic control that remains to be linked with texture. Such an approach opens the way to the identification of specific quantitative trait loci for cell wall determinants of texture and peach shape.

■ ASSOCIATED CONTENT

Supporting Information

Five tables of sugar composition of cell wall material and Student's *t* test statistics. This material is available free of charge via the Internet at http://pubs.acs.org.

■ AUTHOR INFORMATION

Corresponding Author

*Phone: 33 (0)2 40 67 50 63. Fax: 33 (0)2 40 67 50 84. E-mail: marc.lahaye@nantes.inra.fr.

Funding

This work has been supported in part by funds from the program EU FP6 ISAFRUIT (Contract No. FP6-FOOD 016279-2).

Notes

The authors declare no competing financial interest.

■ ACKNOWLEDGMENTS

Part of the work was realized on the instrumental platform BIBS (INRA-Nantes).

■ REFERENCES

(1) Abbott, J. A. Textural quality assessment for fresh fruits and vegetables. *Adv. Exp. Med. Biol.* **2004**, *542*, 265−279.

(2) Harker, F. R.; Redgwell, R. J.; Hallett, I. C.; Murray, S. H.; Carter, G. Texture of fresh fruit. *Hortic. Rev.* **1997**, *20*, 121−224.

(3) Bertin, N.; Borel, C.; Brunel, B.; Cheniclet, C.; Causse, M. Do genetic make-up and growth manipulation affect tomato fruit size by cell number, or cell size and DNA endoreplication? *Ann. Bot. (London)* **2003**, *92*, 415−424.

(4) Mirabet, V.; Das, P.; Boudaoud, A.; Hamant, O. The role of mechanical forces in plant morphogenesis. *Annu. Rev. Plant Biol.* **2011**, *62*, 365−385.

(5) Matas, A. J.; Gapper, N. E.; Chung, M. Y.; Giovannoni, J. J.; Rose, J. K. Biology and genetic engineering of fruit maturation for enhanced quality and shelf-life. *Curr. Opin. Biotechnol.* **2009**, *20*, 197−203.

(6) Seymour, G.; Poole, M.; King, G. J. Genetics and epigenetics of fruit development and ripening. *Curr. Opin. Plant Biol.* **2008**, *11*, 58−63.

(7) Trainotti, L.; Zanin, D.; Casadoro, G. A cell wall-oriented genomic approach reveals a new and unexpected complexity of the softening in peaches. *J. Exp. Bot.* **2003**, *54*, 1821−1832.

(8) Mounet, F.; Moing, A.; Garcia, V.; Petit, J.; Maucourt, M.; Deborde, C.; Bernillon, S.; Le Gall, G.; Colquhoun, I.; Defernez, M.; Giraudel, J. L.; Rolin, D.; Rothan, C.; Lemaire-Chamley, M. Gene and metabolite regulatory network analysis of early developing fruit tissues highlights new candidate genes for the control of tomato fruit composition and development. *Plant Physiol.* **2009**, *149*, 1505−1528.

(9) Tanksley, S. D. The genetic, developmental, and molecular bases of fruit size and shape variation in tomato. *Plant Cell* **2004**, *16*, S181−S189.

(10) Toivonen, P. M. A.; Brummell, D. A. Biochemical bases of appearance and texture changes in fresh-cut fruit and vegetables. *Postharvest Biol. Technol.* **2008**, *48*, 1−14.

(11) Goulao, L. F.; Oliveira, C. M. Cell wall modifications during fruit ripening: when a fruit is not the fruit. *Trends Food Sci. Technol.* **2008**, *19*, 4−25.

(12) Obel, N.; Erben, V.; Schwartz, T.; Kuhnel, S.; Fodor, A.; Pauly, M. Microanalysis of plant cell wall polysaccharides. *Mol. Plant* **2009**, *2*, 922−932.

(13) Westphal, Y.; Schols, H. A.; Voragen, A. G.; Gruppen, H. MALDI-TOF MS and CE-LIF Fingerprinting of plant cell wall polysaccharide digests as a screening tool for arabidopsis cell wall mutants. *J. Agric. Food Chem.* **2010**, *58*, 4644−4652.

(14) Lahaye, M.; Quemener, B.; Causse, M.; Seymour, G. B. Hemicellulose fine structure is affected differently during ripening of tomato lines with contrasted firmness. *Int. J. Biol. Macromol.* **2012**, DOI: 10.1016/j.ijbiomac.2012.05.024.

(15) Galvez-Lopez, D.; Laurens, F.; Quemener, B.; Lahaye, M. Variability of cell wall polysaccharides composition and hemicellulose enzymatic profile in an apple progeny. *Int. J. Biol. Macromol.* **2011**, *49*, 1104−1109.

(16) Dirlewanger, E.; Graziano, E.; Joobeur, T.; Garriga-Caldere, F.; Cosson, P.; Howad, W.; Arus, P. Comparative mapping and marker-assisted selection in Rosaceae fruit crops. *Proc. Natl. Acad. Sci. U.S.A.* **2004**, *101*, 9891−9896.

(17) Haji, T.; Yaegaki, H.; Yamaguchi, M. Inheritance and expression of fruit texture melting, non-melting and stony hard in peach. *Sci. Hortic. (Amsterdam)* **2005**, *105*, 241−248.

(18) Lurie, S.; Crisosto, C. H. Chilling injury in peach and nectarine. *Postharvest Biol. Technol.* **2005**, *37*, 195−208.

(19) Muramatsu, N.; Tanaka, K.; Asakura, T.; Haji, T. Changes in cell wall polysaccharides and physical properties of peach (*Prunus persica* Batsch) fruit during ripening. *J. Jpn. Soc. Hortic. Sci.* **2004**, *73*, 534−540.

(20) Brummell, D. A.; Dal Cin, V.; Crisosto, C. H.; Labavitch, J. M. Cell wall metabolism during maturation, ripening and senescence of peach fruit. *J. Exp. Bot.* **2004**, *55*, 2029−2039.

(21) Brummell, D. A.; Dal Cin, V.; Lurie, S.; Crisosto, C. H.; Labavitch, J. M. Cell wall metabolism during the development of

chilling injury in cold-stored peach fruit: association of mealiness with arrested disassembly of cell wall pectins. *J. Exp. Bot.* **2004**, *55*, 2041−2052.
(22) Zhou, H. W.; Sonego, L.; Khalchitski, A.; Ben-Arie, R.; Lers, A.; Lurie, S. Cell wall enzymes and cell wall changes in 'Flavortop' nectarines: mRNA abundance, enzyme activity, and changes in pectic and neutral polymers during ripening and in woolly fruit. *J. Am. Soc. Hortic. Sci.* **2000**, *125*, 630−637.
(23) Lurie, S.; Zhou, H. W.; Lers, A.; Sonego, L.; Alexandrov, S.; Shomer, I. Study of pectin esterase and changes in pectin methylation during normal and abnormal peach ripening. *Physiol. Plant.* **2003**, *119*, 287−294.
(24) Yoshioka, H.; Hayama, H.; Tatsuki, M.; Nakamura, Y. Cell wall modifications during softening in melting type peach "Akatsuki" and non-melting type peach "Mochizuki". *Postharvest Biol. Technol.* **2011**, *60*, 100−110.
(25) Manganaris, G. A.; Vasilakakis, M.; Diamantidis, G.; Mignani, A. Diverse metabolism of cell wall components of melting and non-melting peach genotypes during ripening after harvest or cold storage. *J. Sci. Food Agric.* **2006**, *86*, 243−250.
(26) Manganaris, G. A.; Vasilakakis, M.; Diamantidis, G.; Mignani, I. Cell wall physicochemical aspects of peach fruit related to internal breakdown symptoms. *Postharvest Biol. Technol.* **2006**, *39*, 69−74.
(27) Yoshioka, H.; Hayama, H.; Tatsuki, M.; Nakamura, Y. Cell wall modification during development of mealy texture in the stony-hard peach "Odoroki" treated with propylene. *Postharvest Biol. Technol.* **2010**, *55*, 1−7.
(28) Karakurt, Y.; Huber, D. J.; Sherman, W. B. Qualtity characteristics of melting and non-melting flesh peach genotypes. *J. Sci. Food Agric.* **2000**, *80*, 1848−1853.
(29) Mohnen, D. Pectin structure and biosynthesis. *Curr. Opin. Plant Biol.* **2008**, *11*, 266−277.
(30) Scheller, H. V.; Ulvskov, P. Hemicelluloses. *Annu. Rev. Plant Biol.* **2010**, *61*, 263−289.
(31) Kurz, C.; Carle, R.; Schieber, A. Characterisation of cell wall polysaccharide profiles of apricots (*Prunus armeniaca* L.), peaches (*Prunus persica* L.), and pumpkins (*Curcubita* sp.) for the evaluation of fruit product authenticity. *Food Chem.* **2008**, *106*, 421−430.
(32) Dirlewanger, E.; Pronier, V.; Parvery, C.; Rothan, C.; Guye, A.; Monet, R. Genetic linkage map of peach [Prunus persica (L.) Batsch] using morphological and molecular markers. *Theor. Appl. Genet.* **1998**, *97*, 888−895.
(33) Hoebler, C.; Barry, J.-L.; David, A.; Delort-Laval, J. Rapid acid hydrolysis of plant cell wall polysaccharides and simplified quantitative determination of their neutral monosaccharides by gas-liquid chromatography. *J. Agric. Food Chem.* **1989**, *37*, 360−365.
(34) Blakeney, A. B.; Harris, P. J.; Henry, R. J.; Stone, B. A. A simple and rapid preparation of alditol acetates for monosaccharide analysis. *Carbohydr. Res.* **1983**, *113*, 291−299.
(35) Blumenkrantz, N.; Asboe-Hansen, G. New method for quantitative determination of uronic acids. *Anal. Biochem.* **1973**, *54*, 484−489.
(36) Ralet, M. C.; Williams, M. A. K.; Tanhatan-Nasseri, A.; Ropartz, D.; Quemener, B.; Bonnin, E. Innovative enzymatic approach to resolve homogalacturonans based on their methylesterification pattern. *Biomacromolecules* **2012**, *13*, 1615−1624.
(37) Ropartz, D.; Bodet, P. E.; Przybylski, C.; Gonnet, F.; Daniel, R.; Fer, M.; Helbert, W.; Bertrand, D.; Rogniaux, H. Performance evaluation on a wide set of matrix-assisted laser desorption ionization matrices for the detection of oligosaccharides in a high-throughput mass spectrometric screening of carbohydrate depolymerizing enzymes. *Rapid Commun. Mass Spectrom.* **2011**, *25*, 2059−2070.
(38) Karas, M.; Ehring, H.; Nordhoff, E.; Stahl, B.; Strupat, K.; Hillenkamp, F.; Grehl, M.; Krebs, B. Matrix-assisted laser-desorption ionization mass spectrometry with additives to 2,5 dihydroxybenzoic acid. *Org. Mass Spectrom.* **1993**, *28*, 1476−1481.
(39) R Development Core Team R: A language and environment for statistical computing. In R Foundation for Statistical Computing, http://www.R-project.org: Vienna, Austria, 2011.
(40) Callahan, A. M.; Scorza, R.; Bassett, C.; Nickerson, M.; Abeles, F. B. Deletions in an endopolygalacturonase gene cluster correlate with non-melting flesh texture in peach. *Funct. Plant Biol.* **2004**, *31*, 159−168.
(41) Zhou, H. W.; Ben-Arie, R.; Lurie, S. Pectin esterase, polygalacturonase and gel formation in peach pectin fractions. *Phytochemistry* **2000**, *55*, 191−195.
(42) Jarvis, M. C.; Briggs, S. P. H.; Knox, J. P. Intercellular adhesion and cell separation in plants. *Plant Cell Environ.* **2003**, *26*, 977−989.
(43) Peaucelle, A.; Braybrook, S. A.; Le Guillou, L.; Bron, E.; Kuhlemeier, C.; Hofte, H. Pectin-Induced Changes in Cell Wall Mechanics Underlie Organ Initiation in Arabidopsis. *Curr. Biol.* **2011**, *21*, 1720−1726.
(44) Ralet, M.-C.; Crepeau, M. J.; Buchholt, H. C.; Thibault, J. F. Polyelectrolyte behaviour and calcium binding properties of sugar beet pectins differing in their degrees of methylation and acetylation. *Biochem. Eng. J.* **2003**, *16*, 191−201.
(45) Pilling, J.; Willmitzer, L.; Fisahn, J. Expression of a Petunia inflata pectin methyl esterase in Solanum tuberosum L-enhances stem elongation and modifies cation distribution. *Planta* **2000**, *210*, 391−399.
(46) Derbyshire, P.; McCann, M.; Roberts, K. Restricted cell elongation in Arabidopsis hypocotyls is associated with a reduced average pectin esterification level. *BMC Plant Biol.* **2007**, *7*, 31.
(47) Brummell, D. A.; Harpster, M. H. Cell wall metabolism in fruit softening and quality and its manipulation in transgenic plants. *Plant Mol. Biol.* **2001**, *47*, 311−340.
(48) Lerouxel, O.; Cavalier, D. M.; Liepman, A. H.; Keegstra, K. Biosynthesis of plant cell wall polysaccharides—a complex process. *Curr. Opin. Plant Biol.* **2006**, *9*, 621−630.
(49) Gunl, M.; Neumetzler, L.; Kraemer, F.; de Souza, A.; Schultink, A.; Pena, M.; York, W. S.; Pauly, M. AXY8 Encodes an alpha-Fucosidase, Underscoring the Importance of Apoplastic Metabolism on the Fine Structure of Arabidopsis Cell Wall Polysaccharides. *Plant Cell* **2011**, *23*, 4025−4040.
(50) Pena, M. J.; Ryden, P.; Madson, M.; Smith, A. C.; Carpita, N. C. The galactose residues of xyloglucan are essential to maintain mechanical strength of the primary cell walls in Arabidopsis during growth. *Plant Physiol.* **2004**, *134*, 443−451.
(51) Maris, A.; Kaewthai, N.; Eklof, J. M.; Miller, J. G.; Brumer, H.; Fry, S. C.; Verbelen, J. P.; Vissenberg, K. Differences in enzymic properties of five recombinant xyloglucan endotransglucosylase/hydrolase (XTH) proteins of Arabidopsis thaliana. *J. Exp. Bot.* **2011**, *62*, 261−271.